A comparison of BGO and BSO crystals used in the dual-readout mode

N. Akchurin [a], F. Bedeschi [b], A. Cardini [c], M. Cascella [d], G. Ciapetti [e], D. De Pedis [f], M. Fasoli [g], R. Ferrari [h], S. Franchino [i], M. Fraternali [i], G. Gaudio [h], J. Hauptman [j], M. Incagli [b], F. Lacava [e], L. La Rotonda [k], S. Lee [j], M. Livan [i], E. Meoni [l], A. Negri [i], D. Pinci [f], A. Policicchio [k,1], F. Scuri [b], A. Sill [a], G. Susinno [k], T. Venturelli [k], C. Voena [f], R. Wigmans [a,*]

[a] Texas Tech University, Lubbock, TX, USA
[b] INFN Sezione di Pisa, Italy
[c] INFN Sezione di Cagliari, Monserrato, CA, Italy
[d] Dipartimento di Fisica, Università di Pisa and INFN Sezione di Pisa, Italy
[e] Dipartimento di Fisica, Università di Roma "La Sapienza" and INFN Sezione di Roma I, Italy
[f] INFN Sezione di Roma I, Italy
[g] Department of Materials Science, Università di Milano-Bicocca, Italy
[h] INFN Sezione di Pavia, Italy
[i] INFN Sezione di Pavia and Dipartimento di Fisica Nucleare e Teorica, Università di Pavia, Italy
[j] Iowa State University, Ames, IA, USA
[k] INFN Cosenza and Dipartimento di Fisica, Università della Calabria, Italy
[l] Institut de Fisica d'Altes Energies (IFAE), Universitat Autonoma de Barcelona, Bellaterra, Barcelona, Spain

ARTICLE INFO

ABSTRACT

We report on a systematic study of the properties of two high-Z scintillating crystals, bismuth germanate (BGO) and bismuth silicate (BSO), in view of the possible application of such crystals in dual-readout calorimeters. Whereas the light attenuation characteristics of both crystals are about the same, BSO offers a considerably higher Cherenkov light yield, and with a given UV filter the separation between the Cherenkov and scintillation signals is substantially better in this crystal.

1. Introduction

High-density scintillating crystals are widely used as calorimeters in particle physics experiments that require excellent energy resolution for electrons and/or photons. However, experiments in which such crystals serve as the electromagnetic (em) section of the calorimeter system usually have poor performance for the detection of hadrons and jets, as a result of their very large e/h ratio [1]. Recently, however, the interest in using such crystals also for the em section of a general-purpose calorimeter system has increased, because of the possibility to separate their signals into Cherenkov and scintillation components. This would open the way to use the crystals as *dual-readout calorimeters*. Event-by-event measurements of the em fraction of showers induced by hadrons or jets, which is possible in such calorimeters, would

eliminate the main reason for the poor hadronic performance [1]. Recent work on this topic has been reported by Auffray et al. [2], Mao et al. [3], Garutti [4] and Gaudio [5].

In a number of earlier papers, we have reported on the possibilities of PbWO$_4$ crystals in this respect [6–9]. These crystals have the advantage of a very low scintillation light yield, which means that Cherenkov photons represent a substantial fraction of the total to begin with. On the other hand, self-absorption of Cherenkov light in these crystals is not insignificant and may be a concern for application in calorimeters where the showers fluctuate over distances of typically 20 cm.

Studies with a BGO crystal showed that it is also possible to separate the two types of light effectively by means of filters, despite the fact that Cherenkov radiation represents only a small fraction of 1% of the light produced in this bright scintillator [10]. Large differences between the spectral properties and the time structure of the two components made this possible. Given these results, it looked attractive to try BSO (bismuth silicate), which has the same crystal structure as BGO (Bi$_4$Si$_3$O$_{12}$), with silicon atoms replacing the germanium ones. In Table 1 some relevant

Table 1
Some relevant properties of BSO and BGO crystals. The light output is normalized to that of NaI(Tl) crystals [11,12].

Crystal	Density ($g\,cm^{-3}$)	Radiation length (mm)	Decay constant (ns)	Peak emission (nm)	Refractive index n	Relative light output
BSO	6.80	11.5	~ 100	480	2.06	0.04
BGO	7.13	11.2	~ 300	480	2.15	0.15

properties of both crystals are compared. These data were compiled on the basis of information obtained in pioneering studies of the calorimetric properties of BSO crystals [11,12].

In this paper, we describe a comparative study of the suitability of BSO and BGO crystals as dual-readout calorimeter media. Two crystals with identical dimensions were tested under exactly the same conditions in a high-energy particle beam at CERN. In Section 2, the crystals and the experimental setup in which they were tested are described, as well as the calibration and data analysis methods that were used. Experimental results are presented in Section 3. In the concluding Section 4, we discuss the implications of these results.

2. Equipment and measurements

2.1. Detectors and beam line

The measurements described in this paper were performed in the H8 beam line of the Super Proton Synchrotron at CERN. Our detectors were high-density crystals of (ortho) bismuth silicate ($Bi_4Si_3O_{12}$, or BSO)[2] and bismuth germanate ($Bi_4Ge_3O_{12}$, or BGO).[3] Both crystals had a length of 18 cm and a cross-section of $2.2 \times 2.2\ cm^2$. This transverse dimension, relevant for our measurements, corresponds to 1.91 radiation lengths (X_0) in the case of BSO and $1.96X_0$ for BGO. The light produced by particles traversing this crystal was read out by two photomultiplier tubes (PMTs) located at opposite ends. Hamamatsu R8900 tubes, with 10 multiplication stages and equipped with a borosilicate window and (on the side intended for detecting the Cherenkov component) a Super Bi-Alkali photocathode, were used for this purpose.

We used different optical transmission filters to study the crystal signals. These filters were 2.5 mm thick, made of glass. Two UV filters, known as UG11 and U330, were intended to increase the relative fraction of Cherenkov light, since they only transmitted light with short wavelengths. A yellow filter (known as GG495), which transmitted only light with wavelengths longer than the 495 nm cut-off value, transmitted almost exclusively scintillation light. The filters were mounted on the two opposite end faces of the crystal, so that light exiting from the left (the L side in Fig. 1) was essentially pure scintillation light, while the light exiting from the R side consisted predominantly of Cherenkov radiation. In order to reduce the light trapping effects of the large refractive index (see Table 1), the PMTs were coupled to the crystal by means of thin Elastocil (silicone) "cookies" ($n = 1.403$). These cookies provided optical contact between the crystal end face and the transmission filter, and between this filter and the PMT window.

Fig. 1. Experimental setup in which the beam tests of the crystals were performed. The angle θ is negative when the crystal is oriented as drawn here.

The crystal was mounted on a platform that could rotate around a vertical axis. The crystal was oriented in the horizontal plane and the rotation axis went through its geometrical center. The particle beam was also steered through this center, as illustrated in Fig. 1. The angle θ, which is frequently used in the following, represents the angle between the crystal axis and a plane perpendicular to the beam line. The angle increased when the crystal was rotated such that the crystal axis L–R approached the direction of the traveling beam particles. The crystal orientation shown in Fig. 1 corresponds to $\theta = -30°$. In several measurements, θ was chosen to be $+30°$, since in that case the probability of detecting the Cherenkov light in PMT R, as well as the Cherenkov content of the signals from this PMT, were maximized.

Two small scintillation counters (TC) provided the signals that were used to trigger the data acquisition system. These trigger counters were 2.5 mm thick, and the area of overlap was $4 \times 4\ cm^2$. A coincidence between the logic signals from these counters provided the trigger. The trajectories of individual beam particles could be reconstructed with the information provided by a small drift chamber (DC), which was installed upstream of the trigger counters. This system made it possible to determine the location of the impact point of the beam particles at the crystal with a precision of about 1 mm. About 25 m downstream of the crystal, placed behind about 20 interaction lengths of material, a $50 \times 50\ cm^2$ scintillator paddle served as a muon counter. The first 10 interaction lengths consisted of the DREAM fiber calorimeter [13,14], which in this study only served to recognize and eliminate beam impurities.

2.2. Data acquisition

Measurement of the time structure of the crystal signals formed a very important part of the tests described here. In order to limit distortion of this structure as much as possible, we used special 15 mm thick low-loss cables to transport the crystal signals to the counting room. Such cables were also used for the signals from the trigger counters, and these were routed such as to minimize delays in the DAQ system.[4] Other signals, e.g., from the muon counter and the calorimeter, were transported through

---

[2] This crystal was one of a batch of nine produced in 2003 by the Futek Furnace Co. in Yokohama, Japan, with the vertical Bridgman method. All these crystals, including the two at our disposal exhibited very similar emission and absorption characteristics.

[3] This crystal was randomly chosen from the thousands of crystals used in the L3 experiment. It was produced around 1985 by the Shanghai Institute of Ceramics with a modified Bridgman method.

---

[4] We measured the signal speed to be $0.78c$ in these cables.

RG-58 cables with (for timing purposes) appropriate lengths to the counting room.

The data acquisition system used VME electronics. A single VME crate hosted all the needed readout and control boards. The signals from the calorimeter channels and the muon counter were integrated and digitized with a sensitivity of 100 fC/count, on 12-bit QDC V792 CAEN modules. The timing information of the tracking chambers was recorded with 1 ns resolution in a 16-bit 16-channel LeCroy 1176 TDC.

The time structure of the calorimeter signals was recorded by means of a Tektronix TDS 7254B digital oscilloscope,[5] which provided a sampling capability of 5 GSample/s, at an analog band-width of 2.5 GHz, over 4 input channels. For the tests described in this paper, only 2 channels were sampled. The oscilloscope gain (scale) was tuned such as to optimize the exploitation of the 8-bit dynamic range, i.e., by choosing the sensitivity such that the overflow rate was $< 1\%$.

The crystal signals were sampled every 2.0 ns, over a total time interval of 1064 ns (532 data points). The time base of the oscilloscope was started by a trigger indicating the passage of a beam particle. Our readout scheme optimised the CPU utilization and the data taking efficiency thanks to the bunch structure of the SPS cycle, where beam particles were provided to our experiment during a spill of 9.6 s, with a repetition period of 48 s. During the spill, all events were sequentially recorded in the internal memory of the scope. We were able to reach, in spill, a data acquisition rate of ~ 500 Hz, limited by the size of the internal scope buffer. No zero suppression was implemented, so that the event size was constant: ~ 1.5 MB, largely dominated by the oscilloscope data.

2.3. Experimental data and analysis methods

We used previously exploited techniques to maximize the scintillation or Cherenkov content of the light detected by the PMTs. These techniques are based on the following differences between the two components:

(1) Differences in *directionality*: Contrary to scintillation light, which is emitted isotropically, Cherenkov light is emitted at a characteristic angle by the relativistic (shower) particles that traverse the detector. By placing the crystal at an angle $\theta = 30°$, the signal measured in PMT R had the largest possible Cherenkov content.
(2) Differences in the *spectral properties*: Cherenkov light exhibits a λ^{-2} spectrum, while the scintillation spectrum of BSO and BGO peaks around 480 nm By using a UV filter, the signal from PMT R was strongly enriched in Cherenkov light.
(3) Differences in *time structure*: Cherenkov light is prompt, while the scintillation mechanism in the crystals is characterized by a decay time of ~ 100 ns (BSO) or ~ 300 ns (BGO). Detailed measurement of the time structure of the R signal made it possible to remove the remaining contaminating scintillation light from the R signals. Details of this method, which was applied to obtain pure Cherenkov signals for all analyses described in this paper, are given in Ref. [10].

Creating a pure scintillation signal (in PMT L) was much easier, because of the fact that scintillation photons outnumbered the Cherenkov ones by three orders of magnitude to begin with. By using a yellow transmission filter, the signals were further purified.

The measurements were performed with a 180 GeV π^+ beam. The angle θ between the crystal axis and the plane perpendicular

to the beam line was varied between $-50°$ and $50°$, in steps of $5°$. At each angle, 30 000 events were collected. In addition, 10 000 randomly triggered events provided pedestal information. For each event, the full time structure of the signals from the two PMTs that read the two sides of the crystal was recorded, as well as the ADC and TDC data from the auxiliary detectors (fiber calorimeter, wire chambers, trigger counters, muon counters).

Off-line, the beam chamber information could be used to select events that entered the crystal in a small (typically 10×10 mm^2) region located around its geometric center. The pion beam contained a few percent of muons and electrons, which could be eliminated with help of the downstream calorimeter and muon counter.

2.4. Calibration of the detectors

The PMTs used in these measurements were calibrated with the 180 GeV pion beam. The calibrations were carried out at $\theta = 30°$, i.e., with the crystal oriented at the Cherenkov angle and the beam hitting the center of the crystal. In this geometry, the most probable energy loss was 22.9 MeV for the BSO crystal, and 24.1 MeV for the BGO crystal, as determined with GEANT-4 Monte Carlo calculations.

For the time structure measurements, no separate calibration effort was performed. We only made sure that the vertical oscilloscope scale was chosen such that no pulse clipping occurred. As the crystals were rotated to larger angles θ, the signals increased and the scale had to be adjusted, e.g., from 100 to 200 to 500 mV full range.

3. Experimental results

3.1. Time structure of the signals

The first topic on which we want to report is the time structure of the signals produced by the light transmitted by the UV filter, U330 in this case.

Fig. 2a shows the average time structure of the signals generated by the 180 GeV pions traversing the BSO and BGO crystals at $\theta = 30°$, on a logarithmic scale. In this way, the difference between the decay constants of the contaminating scintillation light becomes very apparent. Fig. 2b shows the Cherenkov region of the time spectrum in more detail, on a linear scale. Representing the data in this way, it becomes clear that if the Cherenkov signal is chosen by limiting the signals to the interval from 210 to 230 ns, i.e., the shaded area in Fig. 2b, then the contamination of scintillation light is relatively smaller for the signals from the BSO crystal. One factor contributing to this result is the fact that the scintillation light yield in BSO is only 1/4 of that in BGO. The difference between the decay constants (a factor of three) only partially compensates for this.

Another factor comes from the fact that the absolute intensity of the Cherenkov signal is larger for the BSO crystal. This despite the fact that the average energy deposited by the traversing pions in the crystal was a little bit smaller: 65 MeV vs.73 MeV for BSO and BGO, respectively. We come back to this issue in the next section.

3.2. Cherenkov content

The relative purity of the Cherenkov signals observed in PMT R (see Fig. 1) is, apart from the light yield and the decay time of the (strongly dominating) scintillation component, also dependent on the opaqueness of the UV filter for this component, and thus on the details of the emission spectra. Moreover, the relative purity,
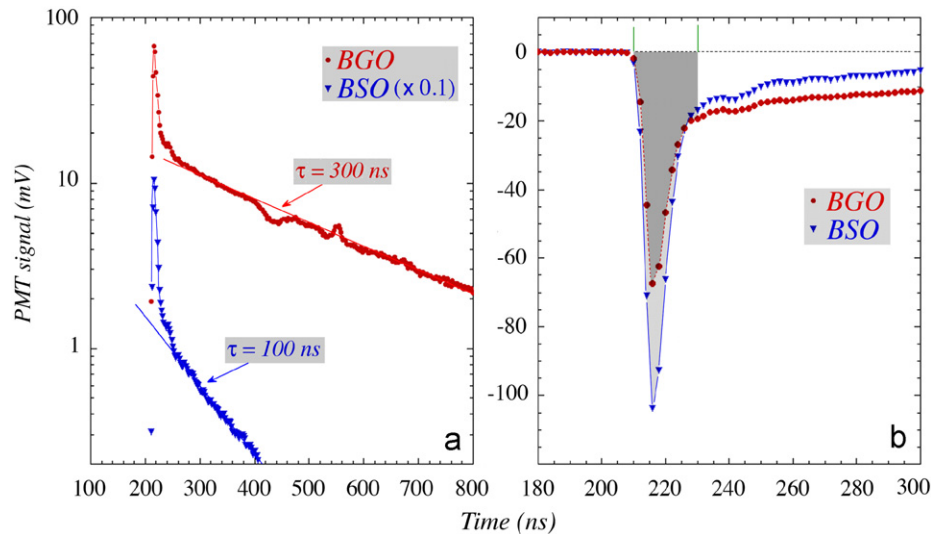
Fig. 2. Average time structure of the signals from light generated by 180 GeV pions traversing the BSO and BGO crystals at $\theta = 30°$, and transmitted by the U330 filter. Results are shown logarithmically for the entire time interval for which these signals were digitized (a), and linearly for the time interval in which the Cherenkov component was detected (b). In order to better illustrate the differences, the BSO signals in the left diagram have been divided by a factor 10.
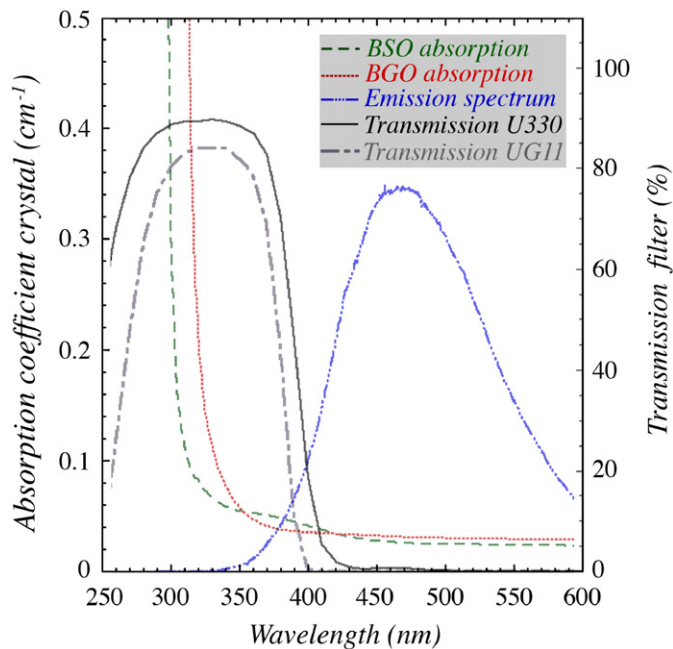
Fig. 3. Emission and absorption spectra (left-hand scale) of the BSO and BGO crystals, and the transmission curve of the U330 and UG11 filters (right-hand scale).

as well as the absolute strength of the Cherenkov signals depend on the absorption characteristics of the crystals.

Fig. 3 shows the emission and absorption spectra of BSO and BGO [15], together with the transmission curves of the U330 and UG11 filters.[6] Whereas the (normalized) emission spectra of these crystals are almost carbon copies of one another, there are significant differences in the absorption characteristics. In particular, the cutoff wavelength is quite different. The absorption coefficient reaches a value of 0.1/cm[7] at 313 nm for BSO, *vs.* 333 nm for BGO.

This difference is of no consequence for the scintillation light, to which the interval 313–333 nm contributes negligibly. However, this interval is very important for the Cherenkov light, whose spectrum is characterized by a λ^{-2} dependence. This difference between the absorption edges thus causes the absolute strength of the Cherenkov signal to be significantly larger for the BSO crystal. It is also partially responsible for the much smaller contamination of scintillation light in the Cherenkov signals.

Detailed analysis of the experimental data shown in Fig. 2 revealed that the signals recorded in the shaded time interval for 180 GeV π^+ traversing the crystals at $\theta = 30°$ contained contributions from scintillation light of 12% in the case of BSO, and 24% for BGO.

Differences in the relative contributions of scintillation light to the signals measured in the shaded time interval also became apparent from the measured angular dependence of the signals generated by the beam pions. These measurements were carried out with a UG11 filter, instead of a U330 one. The main difference between these filters is the fact that UG11 does not transmit any light for wavelengths $\lambda \gtrsim 390$ nm (see Fig. 3). This has the following consequences:

(1) The contamination of scintillation light to the Cherenkov signals is further reduced.
(2) Since the photons with $\lambda > 390$ nm no longer contribute to the Cherenkov signals, the Cherenkov light yield, expressed in photoelectrons per GeV is somewhat smaller for the UG11 filter.
(3) The *ratio* of the Cherenkov light yield in BSO and BGO is further increased in favor of BSO, since the effect of the different short-wavelength cut-off becomes more important.

Fig. 4 shows the time-integrated Cherenkov and scintillation signals as a function of the angle θ at which the 180 GeV beam pions traversed the BSO (Fig. 4a) or BGO (Fig. 4b) crystals. Whereas the scintillation signals are symmetric with respect to perpendicular incidence, the signals detected in PMT R clearly exhibit the characteristics expected from Cherenkov light, which only travels in a direct path to PMT R for values $\theta > 0$. In order to eliminate the effects of the increased path length, and thus isolate the Cherenkov features, we have plotted in Fig. 5 the ratio of the Cherenkov and scintillation signals as a function of the angle of

---

[6] http://www.us.schott.com/advanced_optics/english/index.html.
[7] This corresponds to a light attenuation length of 10 cm.
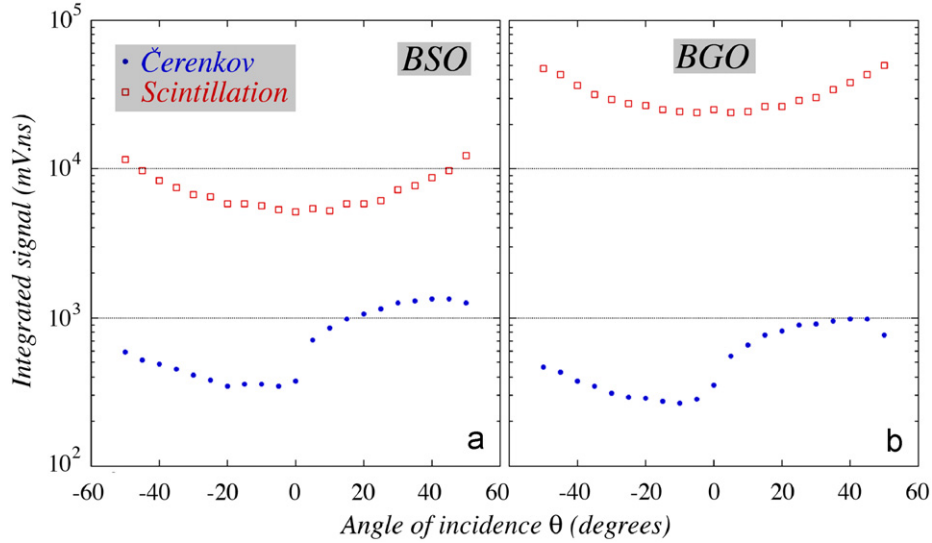
Fig. 4. Angular dependence of the (time integrated) scintillation and Cherenkov signals, for 180 GeV pions traversing the BSO (a) and BGO (b) crystals.
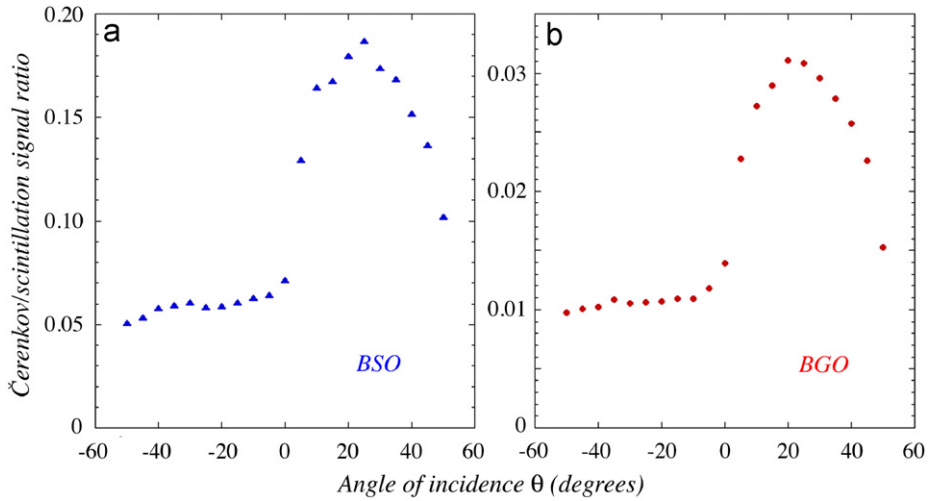
Fig. 5. Angular dependence of the ratio of the (time integrated) Cherenkov and scintillation signals, for 180 GeV pions traversing the BSO (a) and BGO (b) crystals.

incidence of the beam particles. As expected, this ratio reaches a maximum near $\theta = 90° - \theta_C$, where the Cherenkov angle θ_C is $61.0°$ for BSO and $62.3°$ for BGO crystals. Fig. 5 also shows indications for a local maximum near the "anti-Cherenkov angle", $\theta = \theta_C - 90°$, where Cherenkov light emitted in the direction of PMT L and reflected against the end face of the crystal is most likely to be detected in PMT R.

Both Figs. 4 and 5 show that the ratio of Cherenkov and scintillation signals is considerably more favorable for the BSO crystal, although the purity of the Cherenkov signals obtained by correcting the charge collected in the narrow time interval where this light is detected (the shaded area from Fig. 2) for contamination by scintillation light is not much worse in BGO.

3.3. Light attenuation

An important feature, and usually a weak point, of crystals applied in calorimeters is attenuation of the light on its way from the production point to the light detector. At the short wavelengths where the Cherenkov photons are most abundant, this attenuation is typically most significant. This wavelength region is also most vulnerable to the effects of radiation damage.

For these reasons, the attenuation of the Cherenkov light produced in the BSO and BGO crystals had our special attention.

The measurements presented in this subsection were carried out with the UG11 UV filter. This filter selected wavelengths that were on average shorter than those of the U330 filter ($\lambda \lesssim 390$ nm), and therefore these measurements were more sensitive to possible effects of self-absorption.

Fig. 6 shows the average signals generated by the beam particles when they traversed the BSO and BGO crystals at $\theta = 30°$. This angle was chosen so as to maximize the Cherenkov signals. Measurements were carried out at 8 impact points, spread out over the 18 cm long crystals. Results are given separately for the Cherenkov light (Fig. 6a) and scintillation light (Fig. 6b). The location of the PMT's that converted the detected light into electric signals is also indicated. The figure shows that the signals became anomalously large or small when the beam passed the crystal at close proximity of a PMT. However, in the central region of the crystal the characteristics are quite clear:

- The scintillation signals do not depend significantly on the impact point of the beam.
- The Cherenkov signals gradually decrease as the distance the light has to travel to the PMT increases.
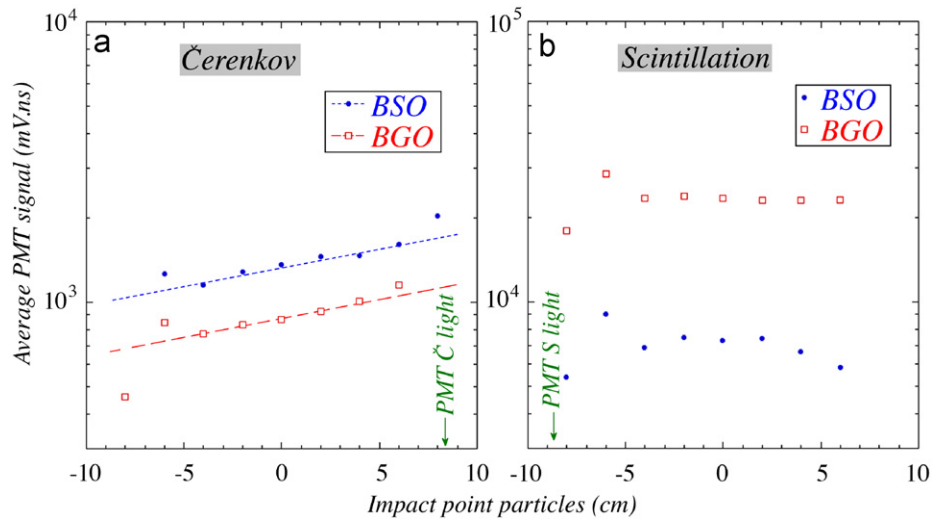
Fig. 6. The average signals generated by 180 GeV pions traversing the BSO and BGO crystals at $\theta = 30°$, as a function of the distance the light had to travel to the PMT that converted the photons into electric signals. Results are given separately for the Cherenkov light (a) and scintillation light (b).
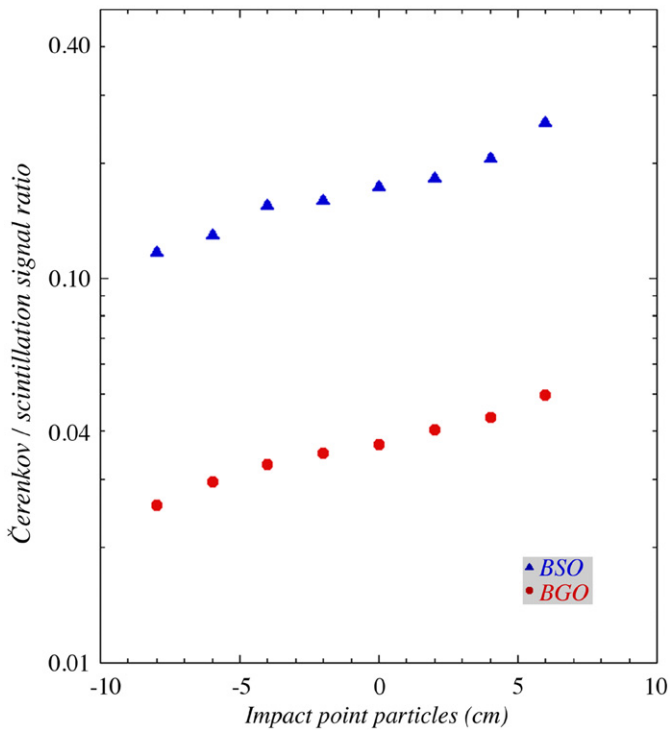
Fig. 7. The ratio of the average Cherenkov and scintillation signals generated by 180 GeV pions traversing the BSO and BGO crystals at $\theta = 30°$, as a function of the impact point of the particles.

- This decrease is *not* significantly different for the two crystals. The dashed lines in Fig. 6a, which are drawn to guide the eye, correspond to an attenuation length of 37 cm.

The latter conclusion is for us the most important one, since we set out to investigate *differences* between these crystals that would be relevant for their application as dual-readout calorimeters. Despite the fact that the BSO is transparent to light with shorter wavelengths than BGO, the increased Cherenkov signals that result from this are *not* subject to stronger attenuation effects, which would make the crystals less suitable in that respect.

This result is also illustrated in Fig. 7, which shows the ratio of the Cherenkov and scintillation signals as a function of the impact point of the beam particles. The relative *changes* in this ratio with the impact point of the particles are indistinguishable between the BSO and BGO crystals. However, as before there is a substantial difference between the absolute values of the ratio, favoring Cherenkov light in the BSO crystal by a factor of five.

3.4. Light yield

One of the main reasons why we started studying high-Z crystals as candidate dual-readout calorimeters was the very low Cherenkov light yield obtained in the fiber calorimeter with which the dual-readout ideas were pioneered: 8–18 photoelectrons per GeV deposited energy, depending on the type of fibers [13]. As a result, fluctuations in the number of (Cherenkov) photoelectrons formed a limiting factor for the hadronic energy of that calorimeter. Non-sampling crystal calorimeters offer the potential of substantially higher light yields, and thus better energy resolution.

The method with which we determined the Cherenkov light yield was based on the assumption that, for a given amount of energy deposited in the crystal, the fluctuations in the numbers of scintillation photons were negligibly small compared to those in the numbers of Cherenkov photons. If this assumption were not entirely valid, then the Cherenkov light yields obtained below would represent in fact a *lower limit*.

Fig. 8 serves to illustrate the method. First, we integrated each scintillation signal over the entire time structure. This integrated charge was used as a measure for the energy deposited by the beam particle (a 180 GeV pion) in the crystal. We used the data obtained at $\theta = 30°$ for this analysis. At this angle, the fraction of *detected* Cherenkov photons reached a maximum.

Monte Carlo simulations showed that, at this angle, the pions deposited on average 65 MeV in the BSO crystal, and 73 MeV in the BGO one. However, these results are very sensitive to nuclear reactions taking place in this process. These resulted sometimes in overflow events, since the oscilloscope scale was chosen to accommodate the much more common events in which no nuclear reactions took place. For this reason, we preferred to use the most probable energy loss of the pions as the basis for the energy calibration. For our setup, this most probable energy loss amounted to 22.9 MeV for BSO and 24.1 MeV for BGO. This result served as the basis for the calibration, and made it possible to
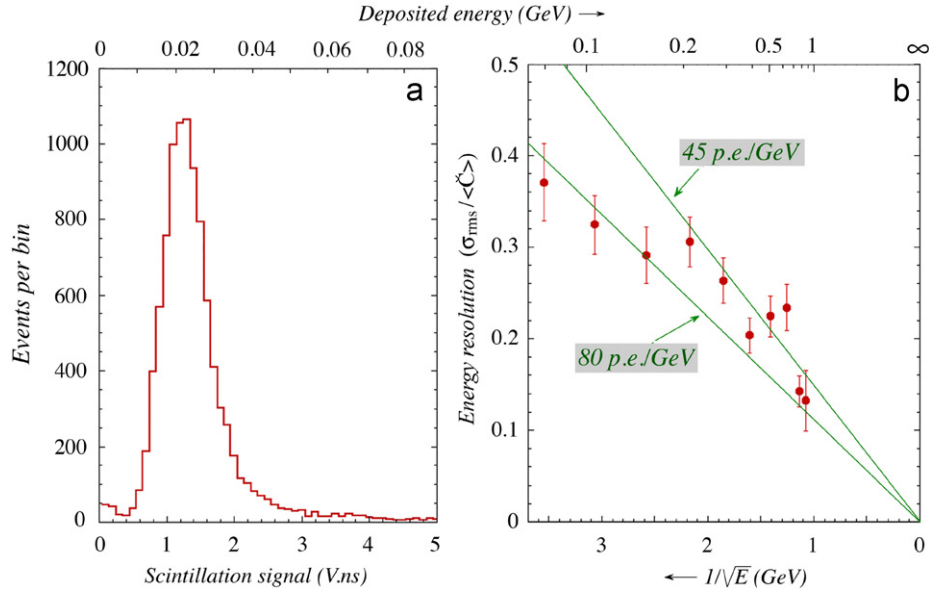
Fig. 8. The scintillator signal distribution for 180 GeV pions traversing the BSO crystal at $\theta = 30°$ (a) and the fractional width of the Cherenkov signal distribution as a function of the amount of energy deposited in the crystal, as derived from the scintillator signal (b).

relate the integrated scintillator signals to the amount of energy deposited in the crystal: 1000 mV ns corresponded to 17.7 MeV. Fig. 8a thus shows the event-by-event distribution of the energy lost by the beam pions.

Unfortunately, the events in the peak of the signal distribution were not suitable for a good measurement of the Cherenkov light yield, since the number of Cherenkov photons was very small for these events. For this purpose, we had to resort to the high-end tail of the distribution, *i.e.*, to events in which at least 80 MeV was deposited in the crystal.

The scintillation signal distribution was subdivided into a number of bins. For each bin, the signal distribution on the *opposite side* of the crystal, *i.e.*, the Cherenkov side, was measured. The fractional width of this distribution, σ_{rms}/C_{mean}, is plotted in Fig. 8b versus the average scintillator signal in this bin, or rather versus the inverse square root of the energy equivalent of this signal ($E^{-1/2}$). The deposited energy itself is indicated by the scale on the top horizontal axis.

If σ_{rms}/C_{mean} scales with $E^{-1/2}$, *i.e.*, if the experimental data points can be fitted with a straight line through the bottom right corner, then the energy resolution is completely determined by (Cherenkov) photoelectron statistics. Because of the very small number of events that was used, it was not possible to obtain a very accurate measurement of the light yield from these data. The two lines drawn in Fig. 8b correspond to light yields of 45 and 80 Cherenkov photoelectrons per GeV deposited energy. It seems a reasonable conclusion that the real value lies somewhere in this interval. This would mean that in the events in which the beam particle acted as a mip, the Cherenkov signals typically consisted of only 1–2 photoelectrons.

However, more important than a precise measurement of the Cherenkov light yield was a comparison of the performance of the BSO and BGO crystals in this respect. Fig. 9 shows the results of this exercise. Events from the tails of the signal distributions (deposited energy > 100 MeV) in these two crystals were analyzed in exactly the same way. We used both runs in which a UG11 filter was used to select the UV light in PMT R, and runs in which a U330 filter was used for this purpose. Despite the fact that only a very small fraction of the events (about 7%) could be used for this purpose, the results were consistent.

The straight lines drawn through the experimental data points in Fig. 9 correspond to a light yield of 48 photoelectrons per GeV
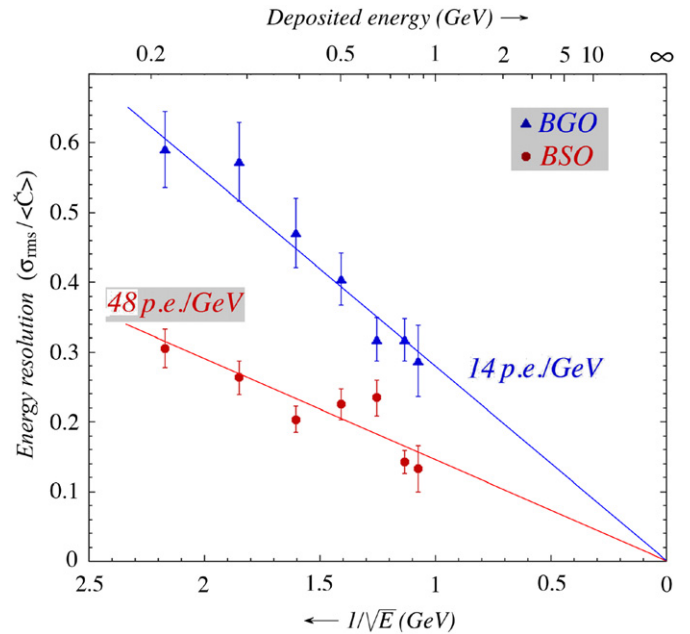
Fig. 9. The fractional width of the Cherenkov signal distribution as a function of the amount of energy deposited in the crystal, as derived from the scintillation signal, for 180 GeV π^+ traversing the BSO and BGO crystals at $\theta = 30°$. The Cherenkov signals were obtained with a UG11 UV filter.

deposited energy for the BSO crystal, *vs.* 14 p.e./GeV for the BGO crystal. The results shown in Fig. 9 concern data in which the UG11 filter was used to select the UV light. The results obtained with the U330 filter indicate, as expected, a slightly larger Cherenkov light yield. For both filters, the Cherenkov light yield was measured to be considerably larger in the BSO crystal than in the BGO one, albeit that the relative difference was somewhat smaller for the U330 filter, commensurate with the factor of about two observed in Fig. 2b.

The described method was used before to measure the Cherenkov light yield of Mo-doped PbWO$_4$ crystals [9] and also for another, tapered BGO crystal [10]. In both cases, beams of 50 GeV electrons were used. These particles deposited on average 10 times more energy in the crystals, which led to much more

accurate measurements. In the case of the BGO crystal, which was equipped with a UG11 UV filter in these measurements, the Cherenkov light yield was measured to be 30 p.e./GeV. The fact that the results found for BGO in the present measurements are lower is probably due to the following factors:

(1) Results obtained with the described method are, strictly speaking, lower limits. This is because they are based on the assumption that the energy deposited in each of the different bins was constant. Fluctuations in the scintillation light yield, combined with the chosen bin widths, increase the fractional widths of the Cherenkov signal distributions shown in Figs. 8b and 9. Because of the very low statistics, the chosen bin widths were much larger in the present experiment, leading to larger fluctuations and thus a smaller estimated Cherenkov light yield.

(2) The relationship between deposited energy and the number of Cherenkov photons produced is different for showering electrons and for the nuclear reactions induced by high-energy pions in the crystals. In particular, the nuclear fragments produced in the collisions and stopped in the crystal are non-relativistic and therefore do not produce any Cherenkov light. However, they do contribute to the scintillation signals and thus to the "measured energy". This effect leads to a lower Cherenkov light yield as well.

3.5. Significance of the results

We should emphasize that the results described here are based on measurements with only one crystal, which was likely produced in a different batch than the one investigated in Ref. [10]. But, as stated earlier, the main purpose of the present study was *not* to measure the Cherenkov light yield as precisely as possible, but rather a comparison between the features of BSO and BGO crystals, when measured under the same circumstances. In that respect, the results of our study were internally consistent and very conclusive.

One may also ask to what extent the age difference, as well as the fact that the BGO crystal has most likely received some radiation exposure during its lifetime, could have affected our results. Irradiation of BGO crystals is known to induce absorption bands in the visible range [16,17]. The position of these bands and their strength is dependent on the quality and purity of the crystal which, in turn, are related to the growing conditions. The irradiation induced absorption bands are not stable [16] and, in some cases, the BGO crystal has been reported to completely recover after a few days [18]. Therefore, considering the absence of absorption bands in the measured optical absorption spectrum of the BGO crystal used in our studies, we believe that the crystal transparency was not significantly affected by aging and previous irradiation.

The shift of the absorption edge that we detected between BGO and BSO (0.20–0.24 eV) is compatible with data reported in the literature [19,20] and further supported by theoretical first-principles calculations [21].

4. Conclusions

We have performed a systematic comparison of two crystals that are considered for application as dual-readout calorimeters: BSO and BGO. Relevant properties in that context include:

- The purity of the Cherenkov signals that can be obtained with UV filters. We found the contamination of scintillation light in

the Cherenkov signals to be smaller by about a factor of two in the BSO crystal.
- The Cherenkov light yield, or rather the number of photoelectrons detected per unit of deposited energy. We measured this yield to be about a factor two to three larger for the BSO crystal.
- The light attenuation length of Cherenkov light. We found the attenuation characteristics of both crystals to be approximately the same.

Given the fact that BSO crystals are also potentially cheaper than BGO, it seems to us that BSO deserves more serious consideration in this context.

We want to point out that a dual-readout calorimeter based on BSO crystals could also benefit from the fact that the experimental information needed for obtaining the strength of the Cherenkov and the scintillation components could be derived from only one signal. Just as for calorimeters based on BGO [22], one could use the time structure of the signals for this purpose (see also Fig. 2). The fact that there is less scintillation light available in the UV filtered signals than for BGO could be (partially) compensated for by using a less selective filter, *e.g.*, UG5 [9].

References

[1] R. Wigmans, New J. Phys. 10 (2008) 025003.
[2] E. Auffray, et al., IEEE Trans. Nucl. Sci. NS-57 (2010) 1454.
[3] R. Mao, et al., IEEE Trans. Nucl. Sci. NS-57 (2010) 3841.
[4] E. Garutti, Nucl. Instr. and Meth. A 628 (2011) 31.
[5] G. Gaudio, Nucl. Instr. and Meth. A 628 (2011) 339.
[6] N. Akchurin, et al., Nucl. Instr. and Meth. A 582 (2007) 474.
[7] N. Akchurin, et al., Nucl. Instr. and Meth. A 593 (2008) 530.
[8] N. Akchurin, et al., Nucl. Instr. and Meth. A 604 (2009) 512.
[9] N. Akchurin, et al., Nucl. Instr. and Meth. A 621 (2010) 212.
[10] N. Akchurin, et al., Nucl. Instr. and Meth. A 595 (2008) 359.
[11] F. Miyahara, et al., Beam test of a BSO calorimeter, Research Report of Laboratory of Nuclear Science, vol. 37, Tohuku University, Japan, 2004, p. 44.
[12] H. Shimizu, et al., Nucl. Instr. and Meth. A 550 (2005) 258.
[13] N. Akchurin, et al., Nucl. Instr. and Meth. A 536 (2005) 29.
[14] N. Akchurin, et al., Nucl. Instr. and Meth. A 537 (2005) 537.
[15] The measurements of the wavelength dependent absorption characteristics of the crystals were performed at the Department of Material Science at the University of Milano-Bicocca, by A. Vedda and M. Fasoli, with a Perkin Elmer Lambda 950 spectrophotometer. The measurements were performed at room temperature, along the crystal length, and were not corrected for effects of reflectivity.
[16] P. Lecoq, P.J. Li, B. Rostaing, Nucl. Instr. and Meth. A 300 (1991) 240.
[17] J.B. Shim, et al., Opt. Mater. 24 (2003) 285.
[18] P. Kozma, P. Kozma Jr., Nucl. Instr. and Meth. A 501 (2003) 499.
[19] M. Ishii, et al., Opt. Mater. 19 (2002) 201.
[20] S. Polosan, A.C. Galca, M. Secu, Solid State Sci. 13 (2011) 49.
[21] M.V. Lalic, S.O. Souza, Opt. Mater. 30 (2008) 1189.
[22] N. Akchurin, et al., Nucl. Instr. and Meth. A 609 (2010) 488.